J Fluoresc (2006) 16:259–265
DOI 10.1007/s10895-006-0098-4

ORIGINAL PAPER

Investigation of a Fluorescence Signal Amplification Mechanism Used for the Direct Molecular Detection of Nucleic Acids

Kim Doré · Mario Leclerc · Denis Boudreau

Received: 7 November 2005 / Accepted: 29 March 2006 / Published online: 2 May 2006
© Springer Science+Business Media, Inc. 2006

Abstract A fluorescence signal amplification mechanism allowing detection limits for DNA in the zeptomolar range was investigated. Photophysical properties of the molecular system were studied in order to better explain the signal amplification that is observed. We show that the confinement of a fluorescent DNA hybridization transducer in aggregates improves its quantum yield and photostability. Furthermore, we show that the combination of the resonance energy transfer occurring within the aggregates with the use of a conjugated polymer as the hybridization transducer and donor allows ultrafast and efficient energy coupling to the aggregates and can lead to the excitation of a large number of acceptors by only one donor.

Keywords Fluorescence signal amplification · Fluorescence resonance energy transfer · Ultrasensitive DNA detection · Orientation and confinement in aggregates · Ultrafast energy transfer

Introduction

The interest for simple yet robust tools for the rapid detection of genetic or infectious diseases, via the recognition of specific sequences of their genome, has grown tremendously in recent years. For example, rapid and accurate detection is essential in order to accurately diagnose pathogenic diseases at the initial stages of an infection [1]. For this purpose, various optical and electrochemical DNA sensors have been proposed [2–13], most of them relying either on complex instrumentation or on some form of chemical amplification (such as the polymerase chain reaction, PCR [14]), or both. We recently reported on the development of an ultrasensitive and sequence-specific DNA detection system that is particularly simple and reliable [10, 15]. This DNA sensor is based on electrostatic interactions between a cationic polymeric optical transducer and a fluorescently tagged negatively charged nucleic acid probe. It was previously reported [10] how this cationic polythiophene transducer, fluorescent in its native random coil configuration, is quenched when it combines with a single-stranded DNA (*ss*DNA) probe to adopt a highly conjugated, planar conformation (hereafter called a "duplex"), but becomes luminescent ($\lambda_{exc} = 420$ nm, $\lambda_{em} = 530$ nm) when a complementary oligonucleotide target is added to this molecular system and the polymer binds in an helical and non-planar configuration (a "triplex") with the negatively charged phosphate backbone of the double-stranded DNA (*ds*DNA) (Fig. 1A). More recently [15], we have shown that tagging the DNA probe with a suitable fluorophore (Fig. 1B) ($\lambda_{exc} = 530$ nm, $\lambda_{em} = 575$ nm) dramatically increases the detection sensitivity: starting with a large number of duplex probes (ca. 10^{10} copies), this sensing system allows the detection of as little as five *ds*DNA copies in 3 mL (3 zM) in the presence of the entire human genome, in only 5 min and without the need for prior amplification of the target.

The model proposed to explain this massive increase in sensitivity involves the formation of aggregates of duplexes in solution, prior to the introduction of the target, which

K. Doré · D. Boudreau (✉)
Chemistry Department and Centre d'optique, photonique et laser (COPL), Université Laval,
Québec, QC, Canada, G1K 7P4
e-mail: denis.boudreau@chm.ulaval.ca

K. Doré · M. Leclerc
Chemistry Department and Centre de recherche en science et ingénierie des macromolécules (CERSIM), Université Laval,
Québec, QC, Canada, G1K 7P4

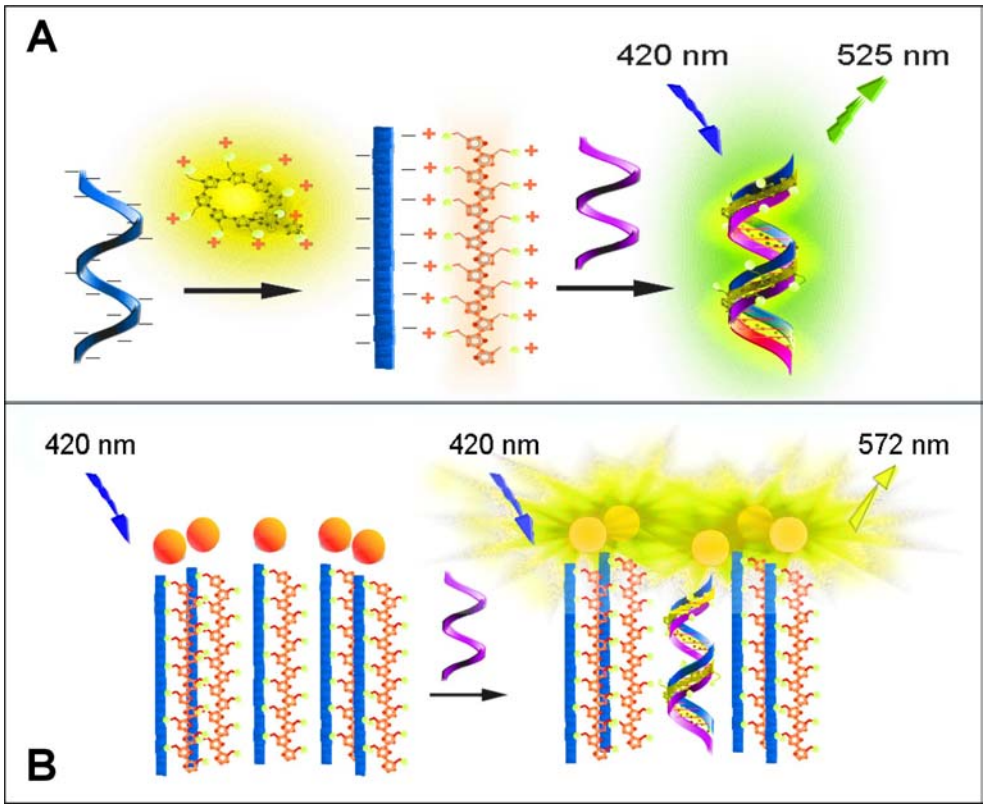

Fig. 1 Schematic representation of the hybridization transduction mechanism for the non labeled (A) and labeled (B) systems

allows resonance energy transfer (RET) among one given donor and a large number of neighboring acceptors, the RET donor being a triplex formed of the DNA double helix and the polymer chain wrapped around it (Fig. 1B). The use of multiple acceptors to amplify the response of optical transducers has been used by other researchers, some of them also for biodetection purposes; however, they described an amplified quenching of the signal, whereas our approach seems to involve a signal amplification more akin to a "superlighting" process [16–18]. As was discussed by Scholes [19], the donors and acceptors in supramolecular aggregates such as these may be close enough to perturb the transition densities of each species and the resulting energy transfer properties. Furthermore, some studies on RET systems localized in micelles [20] or well-structured aggregates [21, 22] show that the confinement of chromophores in specific domains in solutions could help the mechanism of energy transfer, either by decreasing the background from free chromophores [20] or the Förster distance [21], or by increasing the rate of energy transfer [22].

In the present work, photophysical properties were studied by UV–Vis photometry and spectrofluorimetry, in order to investigate the workings of the amplification mechanism process displayed by this molecular detection system. In particular, the energy transfer efficiency and dynamics were measured by frequency-domain spectrofluorimetry. These experiments should shed some light on the mechanisms involved in this optical system and eventually lead to the rational design of a completely new generation of ultrasensitive chemical and biochemical sensors.

Materials and methods

Materials

The polymeric transducer was synthesized according to the procedure previously published [10, 13]. Oligonucleotides were purchased from Integrated DNA Technologies, either labeled or not with Alexafluor 546 (referred to as AF546 in the text). For the sensitivity comparison studies, the DNA capture probe was a 20-mer sequence specific to the *Candida* yeast species, 5′-CAT GAT TGA ACC ATC CAC CA-3′, and the target sequence was its perfect complementary strand 3′-GTA CTA ACT TGG TAG GTG GT-5′ [13]. For all other experiments, the DNA capture probe was a 15-mer sequence specific to the human genomic IVS12 mutation responsible for the hereditary disease *tyrosinemia*, 5′-CCG GTG AAT ATC TGG-3′, and the target sequence was its perfect complementary strand 3′-GGC CAC TTA TAG ACC-5′ [15]. All dilutions and solution handling were performed in sterilized water and plasticware.

Hybridization conditions

For all studies involving DNA hybridization, the polymeric transducer was first mixed with the oligonucleotide probe, and the resulting mixture was diluted in pure water to the desired concentration after an equilibration period of at least 60 s to allow electrostatic complexation. The solution was then heated to 50°C (another 5 min is needed for equilibration) and the target DNA is added. Whereas less than 5 min are needed for hybridization to occur at the concentration level used for the present work ($\sim 10^{-7}$ M of polymer–probe complex), an additional equilibration period of 10 min was added to ensure complete and stable complex formation. For the non labeled system, hybridization was done in 0.1 M NaCl unless specified otherwise; for the labeled system, hybridization was performed in sterilized Nanopure® water. Detailed information on these experimental procedures can be found in references [10, 13] for the non labeled system and in reference [15] for the labeled system.

Determination of fluorescence quantum yield

The quantum yield (QY) of the fluorescent polymeric transducer within the aggregates (or associated with *ds*DNA) was determined using the following formula [23]:

$$\phi_u = \phi_{ref} \times \frac{\text{Afluo}_u}{\text{Afluo}_{ref}} \times \frac{A_{ref}}{A_u} \times \frac{n_u^2}{n_{ref}^2}, \quad (1)$$

where ϕ_u is the QY to be determined and ϕ_{ref} is the QY of the reference; Afluo_u and Afluo_{ref} stand for the area of the fluorescence spectra of the unknown and of the reference, respectively; A_u and A_{ref} represent the absorbance of the unknown and of the reference, respectively; and n_u^2 and n_{ref}^2 are the squared values of the refraction index of the solvent for the unknown and the reference, respectively. Lucifer Yellow, with a QY in water of 0.21 [24] and a peak fluorescence wavelength of 530 nm, was used as the reference. The fluorescence spectra of Lucifer Yellow and of the labeled aggregates (fluorescence maximum at 575 nm, i.e., the peak fluorescence wavelength of AF546) were taken in identical experimental conditions. All fluorescence measurements were recorded on a Varian Cary Eclipse spectrofluorometer. Absorbance measurements were performed at 425 nm (the peak absorption wavelength of both fluorophores) using a custom-made high-stability absorption photometer that allowed the measurement of very low absorbance changes with sufficient accuracy [13]. The instrument is based on a superluminescent blue LED source powered by an ultra low noise current source (Model LDX-3620, ILX Technologies), a photomultiplier tube detector (Model R3896, Hamamatsu) and a low noise current preamplifier (Model SR570, Stanford Research Systems).

Determination of RET efficiency

The RET efficiency (E) can be obtained experimentally according to Eq. (2) [23], where F_{da} is the resulting fluorescence of the donor in presence of the acceptor and F_d the original fluorescence of the donor.

$$E = 1 - \left(\frac{F_{da}}{F_d}\right) \quad (2)$$

Both F_{da} and F_d were measured at 530 nm, the emission maximum of the donor.

Fluorescence lifetime measurements

Fluorescence lifetime measurements were performed using a frequency-domain lifetime spectrofluorometer (Model Fluorolog Tau 3, Horiba Jobin-Yvon). The experiments were done using a 450 W Xenon excitation lamp and a photomultiplier tube detector. The modulation achieved by the Pockell cell and the high-frequency RF amplifiers allowed a frequency modulation range of 5–300 MHz. In order to maximize the detection sensitivity, the emission monochromator was removed from the instrument and measurements were performed either using a highpass (>440 nm) dichroic filter (in which case Fluorescein was used as the lifetime calibration standard) or without any filter (in which case LUDOX® was used as the calibration standard). For each lifetime determination, measurements were taken at at least eight modulation frequencies for an integration time of 10 s, and three replicates were made for each frequency.

Determination of Förster distance, donor–acceptor distance and RET transfer rate

The Förster distance R_0 for a RET system (i.e., the distance at which RET is 50%) is given by:

$$R_0 = 0.211[\kappa^2 n^{-4} \phi_D J(\lambda)]^{1/6} \quad (3)$$

where κ is an orientation factor that varies between 0 and 4 (a value of 2/3 is usually taken for solutions, i.e., without orientation [23]), n is the refractive index (for biological molecules in water, a value of 1.4 is suggested [23]), ϕ_D is the quantum yield of the donor and $J(\lambda)$ is the overlap integral between the donor emission and the acceptor molar extinction coefficient. The average distance between the donor and the acceptor (r) can then be obtained from the following expression:

$$\frac{1}{\tau_{DA}} = \frac{1}{\tau_D} + \left(\frac{1}{\tau_D} \times \frac{R_0^6}{r}\right) \quad (4)$$

where τ_{DA} is the lifetime of the AF546 quenched triplex and τ_D is the lifetime of the triplex. Finally, the transfer rate (k_t) can be obtained by:

$$k_t = \frac{1}{\tau_{DA}} - \frac{1}{\tau_D}$$

Results and discussion

The degree of signal amplification achieved by the labeled molecular system was determined by comparing the signal sensitivity and RSD obtained for labeled and non labeled 20-mer oligonucleotides, using the best experimental conditions found for both systems [13, 15]. The results, presented in Table 1, show that the sensitivity is about 4000 times higher and the RSD on the polymer-probe complex signal (i.e., the blank signal) is seven times lower for the labeled probe system versus the non labeled system. This massive amplification of the detection sensitivity hinges on two conditions: the aggregates must be stable and compact enough to ensure a sufficient proximity between the donor and the acceptors, and the energy transfer between the triplex and the AF546 must allow the excitation of a large number of acceptors with only one donor. Dynamic light scattering has shown that aggregates are formed spontaneously when the polymer-labeled probe duplex is formed. The diameter of these aggregates is on average about 100 nm and remains stable upon hybridization [15]. Assuming that the aggregates are spherical, that *ds*DNA is rod-shaped and has a radius of 9.5 Å and a length of 3.4 Å per base [25], and that the polymer-probe duplex has approximately the same volume (a volume of 5 nm^3 is added for each AF546), a maximum of about 4200 labeled polymer-probe duplexes can fit in a 100 nm diameter spherical aggregate.

In order to confirm the dependence of the increase in signal amplification observed on the large excess of labeled probe-polymer duplexes (versus DNA targets), the fluorescence intensity and QY of the triplex in the aggregates as well as the RET efficiency were measured as a function of the target to probe ratio, i.e., the number of added target *ss*DNA strands (in probe *ss*DNA equivalents), which turns out to be also the number of RET donors in the system (Fig. 2). The results show that the slope of the fluorescence curve is greatest at the smallest target/probe ratios and diminishes rapidly as this ratio is increased. This is in agreement with the expected behavior of our model duplex aggregates, i.e., the relationship between the fluorescence intensity and the number of target copies should only be linear until the number of targets becomes equal, on average, with the number of aggregates. Past this point, the rate of increase in fluorescence will gradually diminish with increasing target concentration, until the increasing fraction of probes that become hybridized within the aggregates threaten the stability of the latter. Measurements by light scattering have shown that, for target/probe ratios higher than 25%, the aggregates collapse and reorganize into smaller entities. In addition, extrapolation of the QY and RET curves towards zero target concentration indicates that the RET efficiency and QY of the aggregates is close to 100% in the range of lowest concentrations. This observation, which could result from the confinement of the AF546 fluorophores and triplex donors within the aggregates and away from quenching species, is consistent with recent studies [26] on the confinement of fluorescent guest molecules (pyrene butyric acid, PBA) in host capsules and the significant increase in fluorescence QY, an effect attributed by the authors to the structural constraint imposed by the host, which minimizes the radiationless decay pathways such as collisional quenching by solvent molecules. Furthermore, Nesterov and coworkers [27] found that the orientation of end-capped polymers within a liquid-crystal phase enhances its intrachain transfer rate and fluorescence QY. In a similar way, our polymer, confined in the aggregates, could also be oriented within them, which could explain the increase of the quantum yield from 3% for the non labeled triplex to around 94% for the labeled aggregates (for a 1% equivalent of target DNA strand). The improved photostability of the triplex fluorophore when placed within the aggregates (100% of conserved fluorescence intensity after 60 min irradiation period versus 40% for the non labeled triplex) is also in agreement with the increase in QY observed in the studies described earlier [26, 27].

Whereas the confinement and orientation of the triplex donor in the molecular aggregates may improve its quantum yield and energy transfer efficiency, the amplification mechanism proposed by our aggregate model must also involve a very fast means to transfer energy between the triplex donor and the AF546 acceptors, in order to explain the massive amplification factor observed. Recent studies on ultrafast intra- and interchain energy transfer in conjugated polymers

Table 1 Detection of *Candida* 20-mer target strand hybridized with labeled or non labeled probe using the polymer as a transducer

Sample	Experimental conditions	Sensitivity (counts/copy)	RSD on the duplex signal (%)
Non labeled probe [13]	50°C, 0.1 M NaCl + 0.3 mM Triton X-100, detection at 530 nm	0.01	3.40
Labeled probe [15]	50°C, pure water, detection at 575 nm	40	0.49

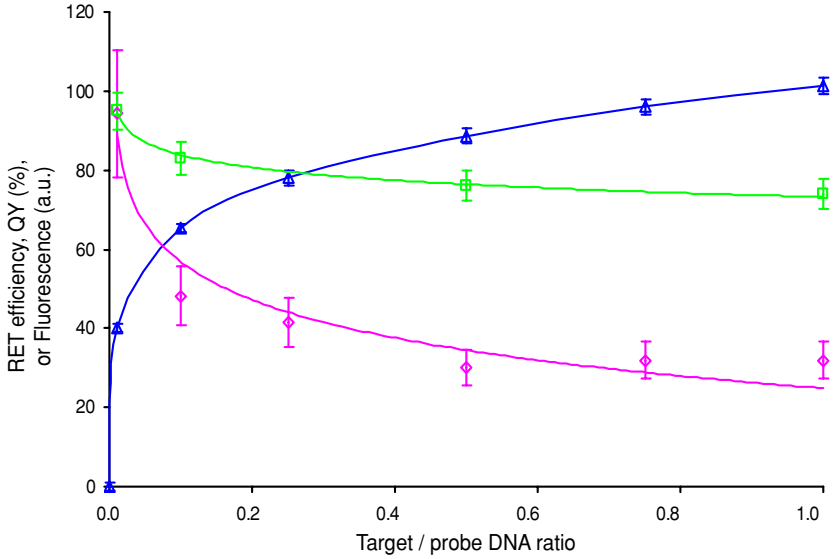

Fig. 2 Fluorescence properties of the amplification system when varying the number of triplex donors (square symbols show the RET efficiency, diamonds show the triplex fluorescence quantum yield in the aggregates, and triangles represent fluorescence intensity)

similar to ours [16–18] mention that the energy transfer occurring in theses molecules might differ from usual Förster-type transfer. This type of energy transfer is indeed ultrafast; Beljonne et al. [16] calculated an interchain transfer rate of 139 ps^{-1} (i.e., each energy hop takes $\sim$7.2 fs) for short polyindenofluorene chains. In view of these studies and of the extremely high detection sensitivity of our sensing system, it is likely that the transfer rate of the triplex donor within the aggregates is also in the ultrafast regime (i.e., excited state lifetimes in femtosecond to picosecond range) to allow the excitation of a large number of AF546 molecules from only one triplex donor.

It has previously been reported [28] that oligothiophenes have fluorescence lifetimes below 1 ns; the measured lifetime of our polythiophene derivative (Table 2, line 1) is thus in agreement with the literature. We also determined that the lifetime of the polymer increases when complexed with *ds*DNA, the donor in the RET system (Table 2, line 2) and decreases drastically, as expected, when associated with the AF546-labeled probe (Table 2, lines 3–6). Interestingly, the τ_A values in lines 3–6 show that the measured lifetime of the AF546 acceptors is influenced by the RET of the donor. In the case of measurement 5, in which the tagged probe and the polymer are in 1:1 stoichiometric concentrations, the lifetime of the AF546 acceptors (1.59 ns) is shorter than the accepted value of 4 ns for the free fluorophore [28], due to the influence on the acceptor decay time of a fast RET rate between the donor and the acceptor [23]. Given

Table 2 Results from multi-exponential analysis of lifetime measurements[a]

Sample	α_T	τ_T	α_A	τ_A	α_S	τ_S	χ^2
1. Polymer alone (with filter)	1	0.17	—	—	—	—	4.21
2. Non labeled triplex in NaCl 0.1 M (without filter)	0.38	0.86	—	—	0.62	≈ 0	0.67
3. AF546 quenched triplex, 10% equivalent of target DNA (with filter), 1.5:1 probe-polymer ratio	0.17	0.01	0.83	3.41	—	—	2.46
4. AF546 quenched triplex, 10% equivalent of target DNA (without filter), 1.5:1 probe-polymer ratio	0.66	0.07	0.15	3.25	0.19	≈ 0	1.1
5. AF546 quenched triplex, 10% equivalent of target DNA (without filter), 1:1 probe-polymer ratio	0.14	0.06	0.21	1.59	0.65	≈ 0	26.7
6. AF546 quenched triplex, 15% equivalent of target DNA (without filter), 1.5:1 probe-polymer ratio	0.76	0.09	0.14	3.94	0.10	≈ 0	3.1

Note. α_T and τ_T (α_A and τ_A, α_S and τ_S) are the proportional coefficient and lifetime for the triplex donor, the AF546 acceptor, and the scatter component, respectively; the χ^2 parameter indicates the goodness-of-fit. For all measurements, uncertainties of 0.5 for the phase (ρ_p) and 0.01 for the modulation (ρ_m) were used.

[a]All lifetimes in ns and taken at 50°C in pure water, unless specified otherwise.

the significant difference in wavelength (>100 nm) between the donor and acceptor absorption bands, we can assume that, for 1:1 stoichiometric conditions, the excitation of the AF546 is only due to RET. In such a case, the more efficient the RET becomes, the greater will be its influence on the decay of the acceptor [29]. This might explain why the acceptor lifetime measured for samples with a higher percentage of hybridized probes (Table 2, line 6) is closer to the lifetime of the free AF546, since the RET of the labeled triplex was shown to decrease with increasing target/probe ratio (Fig. 2). As for the acceptor lifetime values measured at 10% of hybridized probes but with a 1.5:1 excess of tagged DNA probes (Table 2, lines 3 and 4), which is shorter than the lifetime of the free AF546 (3.41 and 3.25 versus 4 ns) but longer than that measured at a 1:1 probe–polymer ratio (1.59 ns), these results were probably influenced by the presence in the aggregates of uncomplexed AF546-labeled probes.

The values presented in Table 2 (obtained with 10% of hybridized probes) were used to calculate the Förster distance R_0 (Eq. (3)). Calculating an overlap integral $J(\lambda)$ equal to 5.601×10^{15} M^{-1} cm^{-1} nm^4 between the triplex emission and the AF546 molar extinction coefficient, we obtained a R_0 of 53 Å for $\kappa = 2$ (a typical value for an oriented system), which falls within the range of 20–90 Å that is usual for molecular systems that display RET properties [23]. In this case, the calculated average distance between the donor and acceptor is 33 Å, which is lower than the Förster distance for the system. From these values, one can finally calculate a RET rate of 1.884×10^{10} transfers per second, or 53 ps per transfer, which is ca. 16 times faster than the emission decay time of 865 ps measured for the non labeled triplex. Faster energy transfers can even be anticipated with a lower degree of hybridization. Thus, the increase in detection sensitivity obtained from the use of labeled probes and the subsequent formation of labeled aggregates could result from the combination of this fast energy transfer between the polymer donor and the AF546 acceptors, the significant increase in the QY of the acceptors, as well as the homotransfer between AF546 chromophores (Stokes shift <20 nm).

Conclusion

The results presented herein on the photophysical properties of our molecular system support the hypothesis of a superlighting process within self-assembled aggregates that provide an enhancement in the fluorescence yield of acceptor molecules and an efficient resonance energy transfer mechanism by conjugated polymer-based donor molecules. The confinement and orientation of the RET donor in these supramolecular aggregates were shown to improve the quantum yield and photostability, while the polymeric, structured, and conjugated nature of the DNA hybridization transducer and its proximity to the multiples acceptors makes possible an ultrafast transfer rate. This important data should contribute to the design of a new generation of ultrasensitive optical biosensors.

Acknowledgements The authors would like to thank Drs. B. Simard and S. Denommée at the Steacie Institute for Molecular Sciences, NRC, Ottawa, Canada, for the lifetime measurements and Dr. H.A. Ho (U. Laval) for the gift of the polymeric transducer and fruitful discussions. K.D. also acknowledges the Natural Sciences and Engineering Council of Canada for a scholarship.

References

1. Daar AS, Thorsteinsdóttir H, Martin DK, Smith AC, Nast S, Singer PA (2002) Top ten biotechnologies for improving health in developing countries. Nat Genet 32:229–232
2. Fodor SPA, Read JL, Pirrung MC, Stryer L, Lu AT, Solas D (1991) Light-directed spatially addressable parallel chemical synthesis. Science 251:767–773
3. Tyagi S, Kramer FR (1996) Molecular beacons: probes that fluoresce upon hybridization. Nat Biotechnol 14:303–308
4. McQuade DT, Pullen AE, Swager TM (2000) Conjugated polymer-based chemical sensors. Chem Rev 100:2537–2574
5. Drummond TG, Hill MG, Barton JK (2003) Electrochemical DNA sensors. Nat Biotechnol 21:1192–1199
6. Storhoff JJ, Lucas AD, Garimella V, Bao YP, Müller UR (2004) Homogeneous detection of unamplified genomic DNA sequences based on colorimetric scatter of gold nanoparticle probes. Nat Biotechnol 22:883–887
7. Nam JM, Stoeva SI, Mirkin CA (2004) Bio-bar-code-based DNA detection with PCR-like sensitivity. J Am Chem Soc 126:5932–5933
8. Liu RH, Yang J, Lenigk R, Bonanno J, Grodzinski P (2004) Self-contained, fully integrated biochip for sample preparation, polymerase chain reaction amplification, and DNA microarray detection. Anal Chem 76:1824–1831
9. Liu B, Bazan GC (2004) Homogeneous fluorescence-based DNA detection with water-soluble conjugated polymers. Chem Mater 16:4467–4476
10. Ho HA, Boissinot M, Bergeron MG, Corbeil G, Dore K, Boudreau D, Leclerc M (2002) Colorimetric and fluorometric detection of nucleic acids using cationic polythiophene derivatives. Angew Chem Int Ed 41:1548–1551
11. Gaylord BS, Heeger AJ, Bazan GC (2002) DNA detection using water-soluble conjugated polymers and peptide nucleic acid probe. Proc Natl Acad Sci USA 99:10954–10957
12. Nilsson KPR, Inganäs O (2003) Chip and solution detection of DNA hybridization using a luminescent zwitterionic polythiophene derivative. Nat Mater 2:419–424
13. Doré K, Dubus S, Ho HA, Levesque I, Brunette M, Corbeil G, Boissinot M, Boivin G, Bergeron MG, Boudreau D, Leclerc M (2004) Fluorescent polymeric transducer for the rapid, simple, and specific detection of nucleic acids at the zeptomole level. J Am Chem Soc 126:4240–4244
14. Saiki RK, Scharf S, Faloona F, Mullis KB, Horn GT, Erlich HA, Arnheim NS (1985) Enzymatic amplification of beta-globin genomic sequences and restriction site analysis from diagnosis of sickle-cell anemia. Science 230:1350–1354
15. Ho HA, Doré K, Boissinot M, Bergeron MG, Tanguay RM, Boudreau D, Leclerc M (2005) Direct molecular detection of nucleic acids by fluorescence signal amplification. J Am Chem Soc 127:12673–12676
16. Beljonne D, Pourtois G, Silva C, Hennebicq E, Herz LM, Friend RH, Scholes GD, Müllen K, Brédas JL (2002) Interchain vs.

intrachain energy transfer in acceptor-capped conjugated polymers. Proc Natl Acad Sci USA 99:10982–10987
17. Klimov VI, McBranch DW, Barashkov NN, Ferraris JP (1997) Femtosecond dynamics of excitons in π-conjugated oligomers: the role of intrachain two-exciton states in the formation of interchain species. Chem Phys Lett 277:109–117
18. Chen L, McBranch DW, Wang HL, Helgeson R, Wuld F, Whitten DG (1999) Highly sensitive biological and chemical sensors based on reversible fluorescence quenching in a conjugated polymer. Proc Natl Acad Sci USA 96:12287–12292
19. Scholes GD (2003) Long-range resonance energy transfer in molecular systems. Ann Rev Phys Chem 54:57–87
20. Vallotton P, Tairi AP, Wohland T, Freidrich-Bénet K, Pick H, Hovius R, Vogel H (2001) Mapping the antagonist binding site of the serotonin type 3 receptor by fluorescence resonance energy transfer. Biochemistry 40:12237–12242
21. Jones GM, Wofsy C, Aurell C, Sklar LA (1999) Analysis of vertical fluorescence resonance energy transfer from the surface of a small-diameter sphere. Biophys J 76:517–527
22. Sautter A, Kaletas BK, Schmid DG, Dobrawa R, Zimine M, Jung G, van Stokkum IHM, de Cola L, Williams RM, Würthner F (2005) Ultrafast energy-electron transfer cascade in a multichromophoric light-harvesting molecular square. J Am Chem Soc 127:6719–6729
23. Lakowicz JR (1999) Principles of fluorescence spectroscopy, 2nd edn. Plenum, New York
24. Stewart WW (1981) Synthesis of 3,6-disulfonated 4-aminonapthalimides. J Am Chem Soc 103:7615–7620
25. Halperin A, Buhot A, Zhulina EB (2004) Sensitivity, specificity, and the hybridization isotherms of DNA chips. Biophys J 86:718–730
26. Dalgarno SJ, Tucker SA, Bassil DB, Atwood JL (2005) Fluorescent guest molecules report ordered inner phase of host capsules in solution. Science 309:2037–2039
27. Nesterov EE, Zhengguo Z, Swager TM (2005) Conjugation enhancement of intramolecular exciton migration in poly(p-phenylene ethynylene)s. J Am Chem Soc 127:10083–10088
28. ISS, Innovations in fluorescence. Website: www.iss.com/Resources/fluorophores.html
29. Maliwal BP, Gryczynski Z, Lakowicz J (2001) Long-wavelength long-lifetime luminophores. Anal Chem 73:4277–4285